



Horizon 2020 Societal challenge 5:
Climate action, environment, resource
efficiency and raw materials

VERIFY

Observation-based system for monitoring and verification of greenhouse gases

GA number 776810, RIA

Deliverable number (relative in WP)	D2.12
Deliverable name:	Final re-analysis of the national scale CO ₂ anthropogenic emissions over 2005-2015
WP / WP number:	WP2
Delivery due date:	Month 42 (31/07/2021)
Actual date of submission:	Month 52 (05/05/2022)
Dissemination level:	Public
Lead beneficiary:	LSCE/CEA
Responsible	LSCE/CEA
Contributor(s):	Audrey Fortems-Cheiney, Grégoire Broquet
Internal reviewer:	Audrey Fortems-Cheiney, Grégoire Broquet

<p style="text-align: center;">Changes with respect to the DoA</p>
<p>1) The final analysis of the national scale CO₂ anthropogenic emissions was supposed to cover 10 years (2005-2015). The period of analysis actually covers a 16-year period from January 2005 to December 2020.</p> <p>2) We deliver this report with a 4-month delay. The main reasons are associated to changes in our plans for the analysis: in particular we decided to use the new TNO-GHGco-v3 inventory (with an update of the emission maps for all the years from 2005 compared to the TNO-GHGco-v2 inventory) as the prior estimate of the NO_x anthropogenic emissions in the new NO_x inversions corresponding to this deliverable. This new inventory was delivered in June 2021 (for years from 2005 to 2018, D2.3) and in July 2021 (for the extrapolation of the previous years into estimates for the years 2019 and 2020, D2.6) and it took time to finalize the preparation of the inversions and conduct them afterwards.</p> <p>3) This analysis should have been based on the assimilation of both NO₂ and CO satellite data. Some experiments, presented in this deliverable, have been conducted to assess the ability to strengthen the fossil fuel CO₂ emissions based on the CO satellite data. It includes a 10-year inversion of the CO emissions based on CO satellite data, and on the derivation of the corresponding anthropogenic CO₂ emissions, from January 2011 to December 2020. However, the conciliation between the results from these experiments and from the NO_x inversions appears to be challenging. Therefore, we had to postpone the statistical synthesis of CO and NO_x inversions and thus the derivation of anthropogenic CO₂ estimates that would be based on the joint assimilation of NO₂ and CO satellite data. Note that we will try to perform such joint assimilation during 2022 as part of the upgrade and extension of the inversions for the joint effort between VERIFY (ending in July 2022) and the CoCO2 projects.</p> <p>4) We aimed at delivering the estimates of the uncertainties in the NO_x, CO and anthropogenic CO₂ emission estimates as part of this new deliverable. The need for such estimates was stressed by the analysis of D2.10 and D2.11, and in the review of D2.11. Such estimates are also required for the statistical synthesis of the CO-based and NO₂-based anthropogenic CO₂ emission estimates. However, the Monte Carlo framework we planned to use to derive these estimates has just been implemented within the Community Inversion Framework (CIF) and is extremely expensive computationally which led us to delay them.</p>
<p style="text-align: center;">Dissemination and uptake (Who will/could use this deliverable, within the project or outside the project?)</p>
<p>This public deliverable should be used within several WPs of VERIFY (WP2, WP3 and WP5) and it will be made available to the public via the VERIFY web-site and its catalogue of products. This study contributes to the international effort to develop atmospheric inverse modeling techniques to quantify the budget and the evolution of fossil-fuel (FF) CO₂ emissions at national scale. In particular, it contributes to the understanding of the potential</p>

of assimilating observations of co-emitted species for this quantification, and to developments for such assimilation.

Short Summary of results (<250 words)

This deliverable presents an update of the atmospheric inversions presented in D2.11. It aims at quantifying monthly to annual budgets of the national emissions of FFCO₂ in Europe over more than a decade. These FFCO₂ emission estimates are based on the assimilation of the long-term series of NO₂ OMI space-borne observations with the new Community Inversion Framework (CIF) and the CHIMERE regional chemistry-transport model. The new set of NO_x inversions covers the period 2005 to 2020. In addition to a temporal extension of the previous analysis, the update includes the use of the newly released TNO-GHGco-v3 inventory instead of the TNO-GHGco-v2 inventory 1) as a prior estimate of the NO_x anthropogenic emissions in the NO_x variational inversions assimilating OMI NO₂ data that corresponds to the first step of the approach, 2) to derive the anthropogenic NO_x to FFCO₂ emission ratios that are used to derive the FFCO₂ emissions in the second step of the approach. The principle of this two-step approach is briefly reminded.

As in D2.11, results mainly indicate an increase of the estimates of anthropogenic NO_x emissions by the inversion compared to the inventory (here TNO-GHGco-v3). As an example, the annual budget of European NO_x anthropogenic emissions is increased by about 3% compared to the TNO-GHGco-v3 inventory in 2015. This correction is slightly lower than that applied to the TNO-GHGco-v2 inventory in D2.11. Overall, all the prior and posterior NO_x anthropogenic emissions presented in D2.11 and D2.12 are very close. As a natural consequence of the increase of the NO_x emissions by the inversion and of the use of the emission ratios from the inventory, the inverted FFCO₂ emissions from the NO_x inversions are larger than those from the TNO-GHGco-v3 inventory, and the differences between these inverted emissions and the inventory are relatively low (below 5% for all annual budgets at European scale). This could be seen as a positive sign of consistency for the years 2005 to 2019. However, the lack of decrease of both the NO_x and NO₂ based FFCO₂ inversion estimate when compared to the inventory for the year 2020 raise concerns since the extrapolation of the TNO-GHGco-v3 inventory for the year 2020 likely significantly underestimates the decrease of the emissions due to the covid-19 crisis (see the explanations and analysis in D2.6).

This deliverable also documents a first attempt at using CO MOPITT data to strengthen the estimate of the monthly to annual scale budgets of the national FFCO₂ emissions, following a two-step approach similar to that when assimilating NO₂ data. It presents a 10-year inversion of the daily European CO emissions at 0.5° resolution for the period 2011-2020 using the TNO-GHGco-v3 inventory as the prior knowledge on these emissions and the CO MOPITT data. Results mainly indicate a slight decrease of the estimates of anthropogenic CO emissions by the inversion compared to the TNO-GHGco-v3 inventory. When this inversion is used to rescale jointly the monthly budgets of sectoral CO and FFCO₂ emissions from the

inventory, it yields FFCO₂ emissions that are smaller than those from the TNO-GHGco-v3 inventory. These differences are relatively weak at national and monthly scales, and the emissions derived from the CO inversion are quite consistent with the TNO-GHGco-v3 inventory, but their sign is opposed to those obtained when assimilating NO₂ data. This demonstrates the need for a better understanding of the uncertainties, and in particular the potential sources of biases in the two inversion processes before attempting at synthesizing the CO and NO₂-based estimates of the FFCO₂ emissions. The previous conclusions from D2.10 and the analysis presented here provide more confidence in the FFCO₂ estimates derived from the NO_x inversions than from the CO inversions.

**Evidence of accomplishment
(report, manuscript, web-link, other)**

- The maps for the monthly values of national FFCO₂ emissions i) corresponding to the NO_x inversions from January 2005 to December 2020, ii) corresponding to the CO inversions from January 2011 to December 2020 are accessible in the VERIFY project database. Note that some of these data may be password protected during a consolidation phase and thus only accessible to the VERIFY partners (via the internal share-point platform).
- A manuscript on the results of the NO_x inversions over the 2005-2020 period is currently written based on D2.11 and the updates reported here. A manuscript on the FFCO₂ emission estimation will be envisaged later.
- D2.11 indicated the submission of two studies documenting developments and analysis that led to the inverse modeling framework presented in the two deliverables D2.11 and D2.12. The two studies are now published:

Fortems-Cheiney, A., Pison, I., Broquet, G., Dufour, G., Berchet, A., Potier, E., Coman, A., Siour, G., and Costantino, L.: Variational regional inverse modeling of reactive species emissions with PYVAR-CHIMERE-v2019, *Geosci. Model Dev.*, 14, 2939–2957, <https://doi.org/10.5194/gmd-14-2939-2021>, 2021.

Fortems-Cheiney, A., Broquet, G., Pison, I., Saunois, M., Potier, E., Berchet, A., et al.: Analysis of the anthropogenic and biogenic NO_x emissions over 2008–2017: Assessment of the trends in the 30 most populated urban areas in Europe. *Geophysical Research Letters*, 48, e2020GL092206. <https://doi.org/10.1029/2020GL092206>, 2021.

-

Version	Date	Description	Author (Organisation)
V0	25/09/2021	Creation/Writing	Audrey Fortems-Cheiney, Grégoire Broquet(CEA)
V0.1	25/11/2021	Writing/Formatting/Delivery	Audrey Fortems-Cheiney, Grégoire Broquet (CEA)
V1	05/05/2022	Formatting/Delivery on the Participant Portal	Philippe Peylin and Aurélié Paquirissamy (CEA/LSCE)

1. Glossary	7
2. Executive Summary	8
3. Introduction	10
4. Data and Method	11
5. Posterior estimate of the NO_x European emissions	14
6. Posterior estimate of the CO European emissions	17
7. Estimation of European FFCO₂ emissions	20
8. Discussion and perspectives for the joint assimilation of NO₂ and CO satellite data	25
9. References	26

1.Glossary

Abbreviation / Acronym	Description/meaning
AMF	Air Mass Factor
BAU	Business As Usual
CC-FF-DASs	Carbon Cycle, Fossil-Fuel, Data Assimilation Systems
CEIP	Centre on Emission Inventories Projection
CIF	Community Inversion Framework
CTM	Chemistry-Transport Model
EMEP	European Monitoring and Evaluation Programme
FF	Fossil-Fuel
GENEMIS	Generation of European Emission Data for Episodes
GNFR	Gridded Nomenclature For Reporting
LULUCF	Land-Use, Land-Use Change and Forestry
MEGAN	Model of Emissions of Gases and Aerosols from Nature
OMI	Ozone Monitoring Instrument
TNO-GHGco	TNO greenhouse gas and co-emitted species (emission inventory)
TVCD	Tropospheric Vertical Column Density
VOC	Volatil Organic Compounds

2. Executive Summary

The uncertainties in national inventories of the FFCO₂ emissions can be significant for some countries in Europe, and large outside Europe. These uncertainties grow when assessing regional to local emissions at subnational scales (Super et al., 2020), and it could grow in time even at the national scale if climate plans lead to major changes in the energy consumption. As for the other types of greenhouse gas (GHG) fluxes, there are thus high expectations regarding the monitoring of the FFCO₂ emissions based on atmospheric "top-down" inversions. CO₂ observation networks dedicated to the monitoring of FFCO₂ emissions are gradually deployed, but so far, there has been a lack of such networks to conduct atmospheric inversions of the FFCO₂ emissions at large scales. The best constant source of atmospheric constraint for the national scale estimate of anthropogenic CO₂ emissions in Europe over more than the past decade probably consists in the satellite measurements of NO₂ and CO, which are "proxy" species co-emitted with CO₂ by the FF combustion.

This D2.12 deliverable presents the work done in the task 2.3 of WP2 in VERIFY for the derivation of the final re-analysis of the FFCO₂ emissions in Europe. This deliverable presents an update of the atmospheric inversions presented in D2.11, based on the NO₂ proxy. The new set of NO_x inversions now covers the period 2005 to 2020. In addition to a temporal extension of the previous analysis, the update includes the use of the newly released TNO-GHGco-v3 inventory instead of the TNO-GHGco-v2 inventory to support these inversions. We also now present the results from CO inversions for the period 2011 to 2020. Note that we will try to perform a joint assimilation of NO₂ and CO later, for the upgrade and extension of our inversions in the frame of the joint effort between VERIFY and the CoCO2 projects.

We derive monthly/national scale budgets of the European fossil fuel CO₂ emissions with a sectoral distribution into five large groups of activity sectors (energy, industry, residential, road transport and the rest of the sectors) from the NO_x inversions or from the CO inversions based on a relatively simple approach. As expected by the increase in posterior NO_x anthropogenic emissions compared to the prior TNO-GHGco-v3 inventory, the national and annual FFCO₂ budgets derived from the NO_x inversions are larger than that of this inventory. On the contrary, the inverted FFCO₂ emissions derived from the CO inversions are smaller than those from the TNO-GHGco-v3 inventory. However, these differences are relatively small at national and monthly scales, the emissions derived from the inversions being quite consistent with the TNO-GHGco-v3 inventory.

This consistency is explained by the fact that the inversion of the NO_x and CO anthropogenic emissions stays relatively close to their prior estimate given by the TNO-GHGco-v3 inventory. This is still a positive indication of the potential of inverse systems to estimate FFCO₂ emissions at the national scale. However, the lack of negative corrections from the NO_x inversions to the inventory in 2020 while this inventory likely underestimates the impact of the covid-19 crisis on the emissions, and the opposite signs of the corrections applied to the inventory by the NO_x and CO inversions raise concerns and questions some of the assumptions underlying our two-step approach for the estimate of FFCO₂ emissions. These points demonstrate the need for a better

understanding of the uncertainties, and in particular the potential sources of biases in the two inversion processes before attempting at synthesizing the CO and NO₂-based estimates of the FFCO₂ emissions using a more advanced approach.

3. Introduction

In Europe, the bottom-up estimates of FFCO₂ emissions are more accurate than that of LULUCF CO₂, CH₄ and N₂O fluxes at national scale. However, the uncertainties in FFCO₂ emission national inventories can be significant for some countries in Europe, and large outside Europe. The uncertainty grows when assessing emission budgets at subnational scales, and it could grow in time even at the national scale if climate plans lead to major changes in the energy consumption (Super et al., 2020). This encourages the development of atmospheric inversion approaches to support the estimate of FFCO₂ emissions at regional scales, which encompass the national scale.

As explained in D2.11, the best constant source of atmospheric constraint for the large-scale estimates of FFCO₂ emissions over more than the past decade probably consists in the satellite measurements of NO₂ and CO, which are “proxy” species mainly co-emitted by the FF combustion. Their sources are approximately collocated in time and space with FFCO₂ sources (Rivier et al., 2006; Suntharalingam et al., 2004; Konovalov et al., 2016), and they have been monitored from space for more than 15 years respectively by the OMI and MOPITT instruments (since 2004 and 2000, respectively). In this context, the task 2.3 of WP2 in VERIFY is dedicated to the development and application of an atmospheric inversion configuration quantifying monthly to annual budgets of the national emissions of FFCO₂ in Europe since 2005 based on the assimilation of the long-term series of spaceborne observations of NO₂ and CO. It relies on the knowledge of the emissions of FFCO₂, NO_x and CO provided by the TNO-GHGco inventories delivered in the task 2.1.

Our inversions target monthly and national scale budgets of the European FFCO₂ emissions with a sectoral distribution into five large groups of activity sectors: energy, industry, residential, road transport and the rest of the sectors. D2.11 and D2.12 document two analyses of the emissions since 2005 based on the assimilation of NO₂ satellite data, following a two-step method detailed in D2.11. While these deliverables initially targeted analysis that extend up to year-1 before their release year, D2.11 covered the period 2005-2019 (the report for D2.11 itself documented results for the period 2008-2017 but estimates for the years 2005-2007 and 2018-2019 were shared in the VERIFY database soon after), and D2.12 covers the period 2005-2020. In addition to the extension in time of the analysis, D2.12 presents other updates compared to D2.11. These updates include the use of the newly released TNO-GHGco-v3 inventory (delivered in June 2021; WP2, Deliverable D2.3; its extrapolation for the years 2019 and 2020 has been delivered in July 2021; WP2, Deliverable D2.6) instead of the TNO-GHGco-v2 inventory (delivered in March 2020; WP2, Deliverable D2.2) to support the different steps of the FFCO₂ emission estimation. Of note is that the extrapolation of the TNO-GHGco-v3 inventory up to the year 2020 partially, but not completely, accounts for the impact of the covid-19 crisis on the emissions. D2.6 provides indications regarding the positive biases likely born by this extrapolation. The inversions were thus expected to provide a different type of difference with this inventory in 2020 compared to the previous ones.

D2.11 and D2.12 initially planned the joint assimilation of satellite CO data together with satellite NO₂ data. A first attempt for such a co-assimilation in the task 2.3 of WP2 of VERIFY has been made by Konovalov and Llova (2018, D2.10), following the approach of Konovalov et al. (2016), to deliver the first fast track inversion of the FFCO₂ emissions in the project. The relatively negative

conclusions from both Konovalov et al. (2016) and Konovalov and Llova (2018) regarding the potential of the assimilation of the CO satellite data for the inversion of the FFCO₂ emissions postponed a first time the use of CO satellite data for our 10+ year analysis from D2.11 to D2.12. We expected that the use i) of CO data from the MOPITT spaceborne instrument (and in particular the MOPITT surface product; Deeter et al., 2019) while Konovalov et al. (2016) and Konovalov and Llova (2018) used CO data from the IASI spaceborne instrument, and ii) of a control resolution of the inversion that is much finer than that of these studies could help overcome the issues they faced when assimilating CO satellite data. But we anticipated the need for series of tests, analysis and adaptation to tackle these issues. This D2.12 documents such tests that were conducted in view to co-assimilate CO satellite data for the analysis of the FFCO₂ emissions. It presents a 10-year CO inversion and the corresponding derivation of a CO-based estimate of FFCO₂ emissions for the period 2011-2020 based on a two-step approach similar to that used with NO₂ data. However, it acknowledges the need for further investigations before providing a FFCO₂ emission estimate based on the synthesis of the inversions assimilating jointly the NO₂ and CO satellite data.

4. Data and Method

As in D2.11, the results documented in this report have been generated with simulations and inversions performed with the new CIF inversion system developed in the VERIFY project (WP3, Deliverable D3.10; Berchet et al., 2021), coupled to a configuration of the regional CTM CHIMERE (Menut et al., 2013) for Europe. However, major updates were implemented in the CIF since the analysis of D2.11 that has been delivered in January 2021. The complexity of the CIF increased with the expansion of its user community. A partial refurbishment and a new standardization of the operations were thus necessary in 2021. The activities in task 2.3 that correspond to D2.11 and D2.12 have kept on supporting the development of the CIF with some specific implementations and tests which were connected to the CO and NO₂ satellite data assimilation.

D2.11 provides detailed rationale and description for the approach to derive FFCO₂ emissions from NO_x or CO satellite data. This new report reminds its main principles. While this approach has been used in effect to produce the 16-year analysis of national scale FFCO₂ emissions in Europe when using NO₂ data, it has only been partially explored when using CO data. The concept for the joint assimilation of NO_x and CO data is discussed in the conclusion.

4.1 Configuration of CHIMERE for the simulation of NO₂ and CO concentrations in Europe

Here, the configuration of the atmospheric chemistry transport CHIMERE for Europe is almost the same as in D2.11. In the simulations corresponding to this deliverable, CO was already simulated together with NO_x and other species that are connected to them through the chemical scheme. The main characteristics of this configuration are briefly reminded in Table 2. However, of note is that the wet deposition was not implemented in the CIF-CHIMERE system at the time of Deliverable D2.11. This is corrected and now implemented.

The chemical scheme used in PYVAR-CHIMERE is MELCHIOR-2, with more than 100 reactions [CHIMERE 2017], including 24 for inorganic chemistry. Climatological values from the LMDZ-INCA global model [Szopa et al., 2008] are used to prescribe concentrations at the lateral and top boundaries and the initial atmospheric composition in the domain. Considering the NO₂ short lifetime, we do not consider its import from outside the domain: its boundary conditions are set to zero. Nevertheless, the lateral and top boundaries for other species such as ozone O₃, nitric acid HNO₃, peroxyacil nitrates PAN, formaldehyde HCHO, participating to the NO_x and/or to the CO chemistry, are taken into account.

Domain	Europe (15.25°W-35.75°E; 31.75°N-74.25°N)
Horizontal resolution	0.5°×0.5° regular grid
Vertical resolution	17 layers, from the surface to 200hPa
Meteorological fields	ECMWF operational meteorological forecast (Owens and Hewson, 2018)
Chemical scheme	MELCHIOR-2
Fixed or prior estimate of the boundary conditions	Climatological values from the LMDZ-INCA global model (Szopa et al., 2008)

Table 2. Main characteristics of the CHIMERE configuration.

4.2 Prior estimate of the anthropogenic and biogenic emissions

The prior estimate of the anthropogenic NO_x and CO emissions is derived from the new TNO-GHGco-v3 gridded inventory for the period 2005- 2018 (WP2, Deliverable D2.3), based on the last EMEP/CEIP official country reporting for air pollutants. The emissions for the years 2019 and 2020 have been extrapolated by applying an in-sample approach. The extrapolation technique for the year 2020 takes into account the impacts of the lockdowns due to covid-19 to some extent. Nevertheless, these impacts are underestimated with the proxy data used in the extrapolation (Deliverable D2.6). The impact on NO_x emissions is indeed between 0 and -6% for individual countries whereas it is estimated to be -3 and -13% with the weight factors from the CAMS_COP079 project, applying country-, and sector-specific temporal weight factors (WP2, Deliverable D2.6). It should also be noted that we have not made a specific set up of the temporal correlations or of the resolution of the control vector for 2020 even though the typical diurnal cycles used to derive hourly emissions from the TNO-GHGco-v3 for all years is probably biased for this year (WP2, Deliverable D2.6).

CO biogenic emissions are assumed to be negligible and are not taken into account. The fixed anthropogenic emissions for VOCs are still obtained from the EMEP inventory (Vestreng et al., 2005; EMEP/CEIP website). Prior biogenic NO_x and fixed VOCs emission estimates still come from the MEGAN model (Guenther et al., 2006).

4.3 Satellite observations

The NO₂ OMI-QA4ECV satellitedata (Boersma et al., 2017; Levelt et al., 2018) are used for the NO_x inversion in a way similar to that in D2.11.

The CO inversion experiments of this new deliverable D2.12, use the CO data from the MOPITT instrument (Deeter et al., 2019). MOPITT has been flown onboard the NASA EOS-Terra satellite, on a low sun-synchronous orbit that crosses the Equator at 10:30 and 22:30 LST. The spatial resolution of its observations is about 22×22 km² at nadir. It has been operated nearly continuously since March 2000. MOPITT CO products are available in three variants: thermal-infrared TIR only, near-infrared NIR only and the multispectral TIR-NIR product, all containing total columns and retrieved profiles (expressed on a 10-level grid from the surface to 100 hPa). We choose to constrain CO emissions with the MOPITT “surface” product. Among the different MOPITTv8 products, we choose to work with the multispectral MOPITTv8-NIR-TIR one (also called MOPITT-v8J), as it provides the highest number of observations, with a good evaluation against in situ data from NOAA stations (Deeter et al., 2019). Following an approach similar to that of the assimilation of OMI NO₂ data into the NO_x inversions, the MOPITTv8-NIR-TIR surface concentrations are subsampled within each model grid cell into single “super-observations”: we selected the median of each subset of MOPITTdata within each 0.5°×0.5° grid cell and each physical time-step (about 5–10 min).

4.4 Separate variational inversion of the NO_x and CO emissions

The inversions of the NO_x or CO emissions consist in correcting the "prior" estimate of these emissions and of the model initial and/or boundary conditions to improve the fit between CHIMERE and the satellite NO₂ or CO data, respectively. Fortems-Cheiney et al. (2021a) provides details on the principle and configuration for these inversions. The optimal ("posterior") estimate of the emissions in a statistical sense is found by iteratively minimizing the following cost function $J(\mathbf{x})$:

$$J(\mathbf{x}) = \frac{1}{2} (\mathbf{x} - \mathbf{x}^b)^T \mathbf{B}^{-1} (\mathbf{x} - \mathbf{x}^b) + \frac{1}{2} (\mathbf{H}(\mathbf{x}) - \mathbf{y})^T \mathbf{R}^{-1} (\mathbf{H}(\mathbf{x}) - \mathbf{y})$$

As in D2.11, series of 1-day inversion windows are conducted for NO_x and then combined to provide an estimate of the NO_x emissions over the whole period of analysis.

The control vector \mathbf{x} contains the variables to be optimized by the NO_x inversion:

- the NO and NO₂ anthropogenic emissions at a 1-day temporal resolution, at a 0.5° ×0.5° (longitude, latitude) resolution and over the first 8 vertical levels of our regional CTM CHIMERE (see Section 1.2), i.e. for each of the corresponding 101×85×8 grid cells,
- the NO biogenic emissions at a 1-day temporal resolution, at a 0.5° ×0.5° (longitude, latitude) resolution and at the surface (over 1 vertical level only), i.e. for each of the corresponding 101×85×1 grid cells,
- the daily NO and NO₂ 3D initial conditions at 0:00 UTC, at a 0.5° ×0.5° (longitude, latitude) resolution and over the 17 vertical levels of CHIMERE.

For CO, series of 1-month inversion windows are conducted. The control vector \mathbf{x} for CO inversions is currently very similar to that for the NO_x inversions (see Fortems-Cheiney et al. 2021a for more details). However, due to the relatively long lifetime of CO, we have to account for the CO lateral boundary conditions at the borders of the CHIMERE domain and for the uncertainties in these conditions. In addition, the chemical production of CO by VOCs is fixed and not controlled here by the inversion. Therefore, the control vector for the CO inversions contains:

- the CO anthropogenic emissions at a 1-day temporal resolution, at a 0.5° × 0.5° (longitude, latitude) resolution and over the first 8 vertical levels of CHIMERE, i.e. for each of the corresponding (30 or 31 days) × 101 × 85 × 8 grid cells,
- the CO lateral boundary conditions a 1-day temporal resolution, at a 0.5° × 0.5° (longitude, latitude) resolution, i.e. for each of the corresponding (30 or 31 days) × 372 grid cells, over the 17 vertical levels of CHIMERE,
- the CO 3D initial conditions at 0:00 UTC the first day of the month, at a 0.5° × 0.5° (longitude, latitude) resolution and over the 17 vertical levels of CHIMERE.

The uncertainties in the observations \mathbf{y} together with that in the observation operator H (i.e. the model CHIMERE linking the control variables to the observed concentrations), and the uncertainties in the prior estimate of the control vector \mathbf{x}^b are assumed to have a Gaussian distribution and are thus characterized by their covariance matrices \mathbf{R} and \mathbf{B} , respectively. The assumptions made to define these matrices have been detailed in D2.11 and in Fortems-Cheiney et al. (2021a) and the main features for the parts of \mathbf{B} corresponding to the surface emissions are recalled in Table 1.

	Anthropogenic emissions	Biogenic emissions
NO _x	50% at 0.5° × 0.5° and daily scale Spatial correlations of 50km No day to day temporal correlation	100% at 0.5° × 0.5° and daily scale Spatial correlations of 50km
CO	100% at 0.5° × 0.5° and daily scale Spatial correlations of 50km No day to day temporal correlation	-

Table 1. Assumptions used for deriving the covariance matrix of the uncertainty in the prior estimate of the NO_x and CO emissions.

5. Posterior estimate of the NO_x European emissions

The main behavior of the NO_x inversions here is similar to that in the first analysis presented in D2.11. In particular, D2.11 provided details on the fit to the assimilated data, on the lack of constraints for the inversion during autumn and winter, and on the lack of sensitivity between the

NO₂ tropospheric columns and the NO_x emissions, at least over rural areas. This section focuses on the results from the NO_x inversions only in terms of comparisons between the posterior NO_x anthropogenic emission estimates from the new analysis and from D2.11, and the TNO-GHGco-v2 and TNO-GHGco-v3 estimates, since January 2005.

As seen in Figure 1, the TNO-GHGco-v3 monthly budgets are very close to the TNO-GHGco-v2 ones from 2005 to 2017. Differences for the year 2018 and for year 2019 can be explained by the fact that the estimates for these years have been extrapolated from by applying an in-sample approach in the TNO-GHGco-v2 inventory (Deliverable D2.4) whereas in the TNO-GHGco-v3 inventory i) the estimate for the year 2018 is based on the last EMEP/CEIP official country reporting for air pollutants (Deliverable D2.3) and ii) the estimate for the year 2019 has been extrapolated with an updated in-sample approach (with minor adjustments to the extrapolation methodology and the inclusion of additional source sectors as explained in Deliverable D2.6).

The inversion estimates from the new analysis are also very close to that from D2.11. In both analyses, the inversion mainly applies positive increments to the TNO-GHGco-v2 or TNO-GHGco-v3 prior anthropogenic emission estimates in spring and in summer (Figure 1). Nevertheless, probably due to improvements related to the CIF system (i.e., vertical interpolation, wet deposition) or to the upgrades from the TNO-GHGco-v2 inventory to the TNO-GHGco-v3 inventory, the increments are slightly lower in the new analysis (Table 1). With the new analysis, in 2015, the posterior anthropogenic emission estimates for France, Germany, Italy, Poland and Spain are about +3.6%, +4.9%, +5.8%, +1.3%, and +5.0% higher than the prior ones, respectively (Table 3), indicating that the prior TNO-GHGco-v3 European NO_x emissions could be slightly underestimated. Posterior anthropogenic emission estimates are about +2.9 % higher than the prior ones for the entire modeling domain in 2015 (Table 3). This is still in line with the 2005-2014 average difference of +3.9% between the prior and posterior European emission estimates documented by Miyazaki et al., (2017).

Unlike D2.11, the new analysis covers the year 2020. Prior anthropogenic emissions, taking partially into account the impacts of COVID-19 and lockdowns (WP2, Deliverable D2.6), are strongly lower in 2020 than in 2019. Since the impact of the lockdowns are underestimated with the proxy data used in the extrapolation of the TNO-GHGco-v3 inventory for 2020 (Deliverable D2.6), we would have expected negative increments from the inversions for this year. However, the inversions still results in positive increments, even if these increments are slight and lower in spring 2020 than for the other years (e.g., Figure 1, Table 4). It could be explained to some extent by the fact that we have not used a specific set up of the temporal correlations or of the resolution of the control vector for 2020 even though the typical diurnal cycles used to derive hourly emissions from the TNO-GHGco-v3 for all years is probably biased for this year (WP2, Deliverable D2.6). In addition, as already discussed in Fortems-Cheiney et al. (2019) and in D2.11, the low increments applied to the inventory can be explained by strong non-linear relationships existing between the NO_x emissions and the satellite NO₂ columns (Lamsal et al., 2011; Vinken et al., 2014; Miyazaki et al., 2017; Li and Wang, 2019). Further work is required to understand these non-linearities.

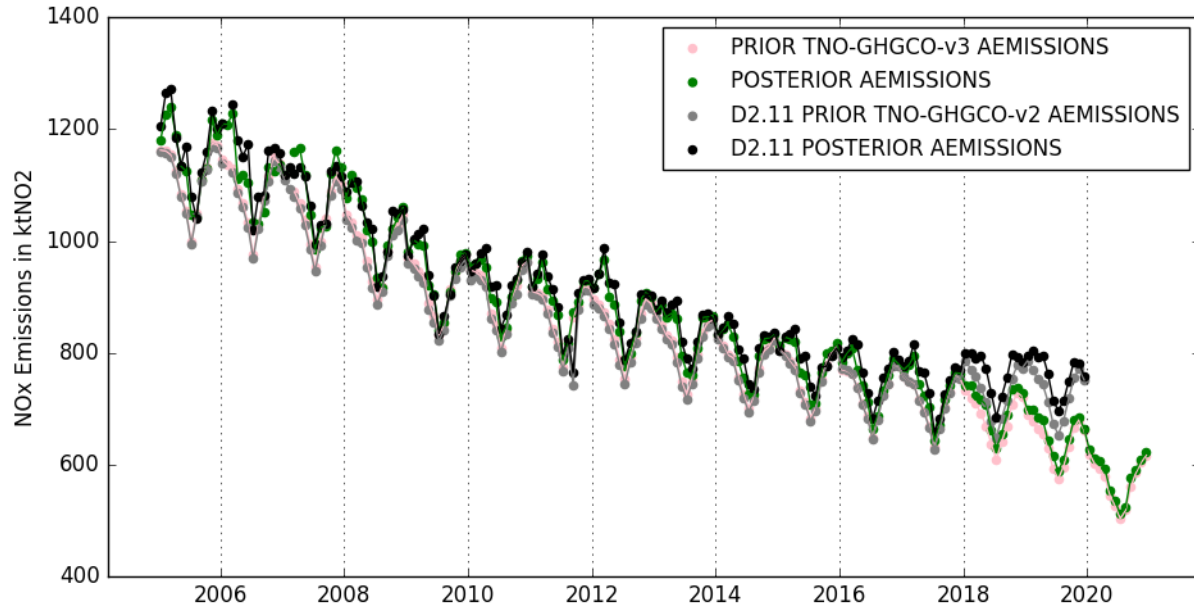


Figure1. Monthly estimates of anthropogenic NO_x prior emissions from the TNO-GHGco-v3 inventory (in pink) and posterior anthropogenic emission estimates (in green), for the continental domain, in ktNO₂, and for the period January 2005 to December 2020. Monthly estimates of anthropogenic NO_x prior emissions from the TNO-GHGco-v2 inventory (in grey) and posterior anthropogenic emission estimates for the period January 2005 to December 2019 from D2.11 (in black) are also shown.

<i>Annual and national prior TNO-GHGco and posterior NO_x anthropogenic emission estimates in 2015</i>						
Country	<i>Prior TNO-GHGco-v2</i>	<i>Posterior from D2.11</i>	<i>Increments in %</i>	Prior TNO-GHGco-v3	Posterior	Increments in %
France	811	866	+6.2	803	832	+3.6
Germany	1214	1305	+7.4	1329	1394	+4.9
Italy	569	633	+11.4	513	562	+5.8
Poland	666	694	+4.3	661	670	+1.3
Spain	566	617	+8.9	560	588	+5.0
Entire domain	13034	13716	+5.2	13073	13457	+2.9

Table 3. in bold: Annual and national prior TNO-GHGco-v3 and posterior NO_x anthropogenic emission estimates in ktNO₂, and the corresponding relative increments from the inversion in %, for the year 2015. In italic: estimates from the TNO-GHGco-v2 inventory and from the inversions presented in the D2.11 deliverable together with the corresponding increments.

<i>National prior TNO-GHGco and posterior NO_x anthropogenic emission estimates in spring 2015</i>	<i>National prior TNO-GHGco and posterior NO_x anthropogenic emission estimates in spring 2020</i>
--	--

Country	Prior TNO-GHGco-v3	Posterior	Increments in %	Prior TNO-GHGco-v3	Posterior	Increments in %
France	204	215	5.1	133	135	1.5
Germany	336	364	8.3	247	259	4.6
Italy	135	150	11.0	87	92	5.8
Poland	167	170	1.8	149	151	1.5
Spain	142	149	5.3	90	91	1.3
Entire domain	3302	3458	4.7	1902	1942	2.1

Table 4. National prior TNO-GHGco-v3 and posterior NO_x anthropogenic emission estimates in ktNO₂, and the corresponding relative increments from the inversion in %, for spring 2015 and spring 2020.

6. Posterior estimate of the CO European emissions

This section focuses on the results from the 10-year CO inversion for the period 2011 to 2020. The CHIMERE prior simulation nearly systematically overestimates the CO concentrations compared to the MOPITT “surface” super-observations (for example in February 2015, Figure 2). Consequently, the inversion applies negative increments to the CO prior anthropogenic emission estimates (Figure 3 and Figure 5), particularly over large cities and over Central Europe (Figure 3). By construction, the inversions bring the CHIMERE CO concentrations closer to the MOPITT “surface” super-observations, mainly over large cities and over industrial areas (e.g., over the Po Valley, over the Benelux, over southwestern Poland, Figure 4). It is worth stressing that the posterior simulation still presents positive biases compared to the observations. It can be due to the fact that the anthropogenic signal in the spatial variations of the measured CO columns may come mostly from the a priori CO columns employed in the MOPITT retrieval procedure, as discussed by Konovalov et al. [2016] with IASI satellite data. As demonstrated by sensitivity tests (not shown), there is a low sensitivity to the anthropogenic CO emissions of the satellite CO measurements, and, since we have applied the averaging kernel (AK) and the prior MOPITT profile to our CHIMERE simulations, of our simulated concentrations.

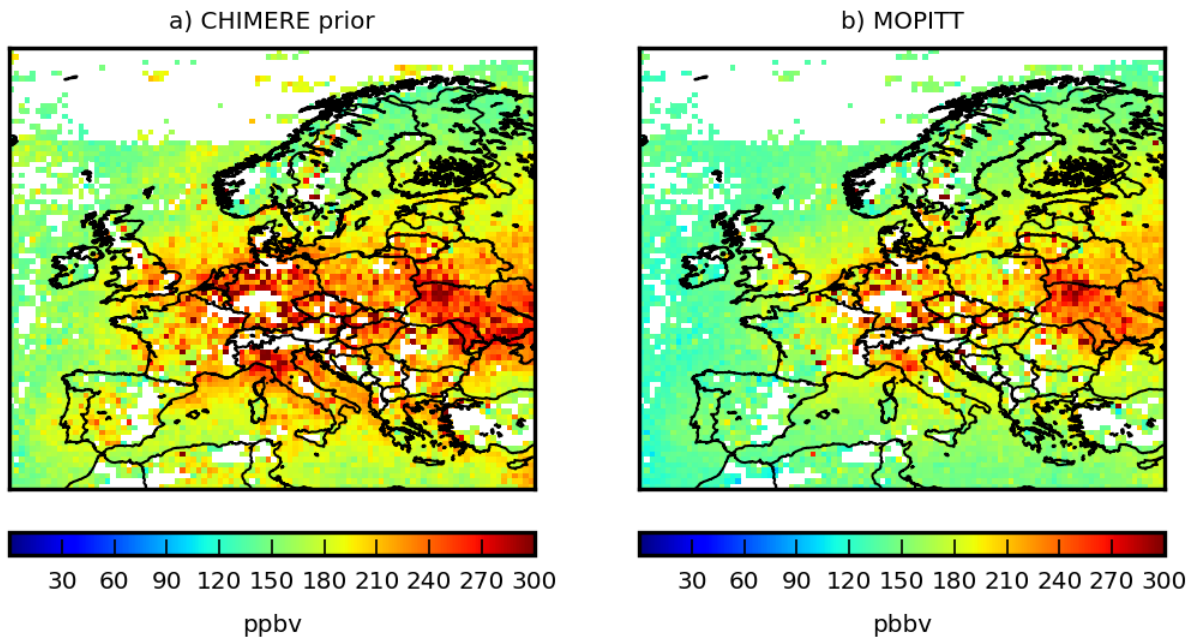


Figure 2. Averages of the CO concentrations a) simulated by CHIMERE using the prior TNO-GHGco-v3 anthropogenic emission estimate where and when MOPITT-v8J “surface” super observations are available, and b) observed by MOPITT-v8J, in ppbv, at the 0.5°x0.5° grid-cell resolution, in February 2015.

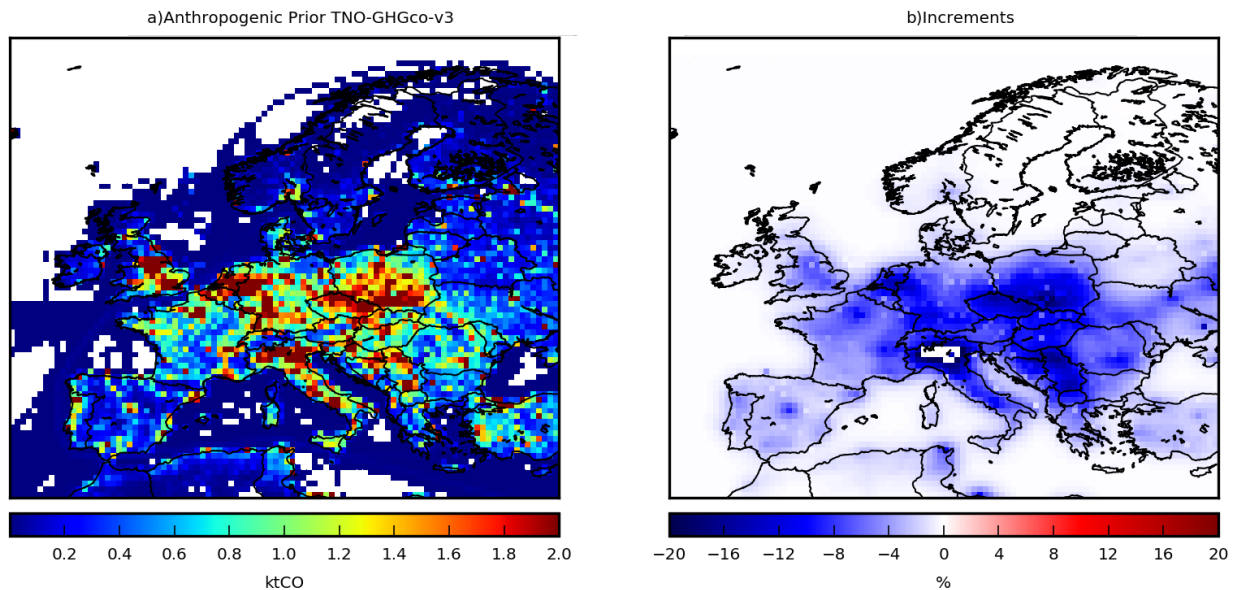


Figure 3. a) Monthly budget of CO emissions per model grid-cell, in ktCO, and b) monthly mean relative increments to the TNO-GHGco-v3 inventory of CO anthropogenic emissions from the inversion, in %, in February 2015.

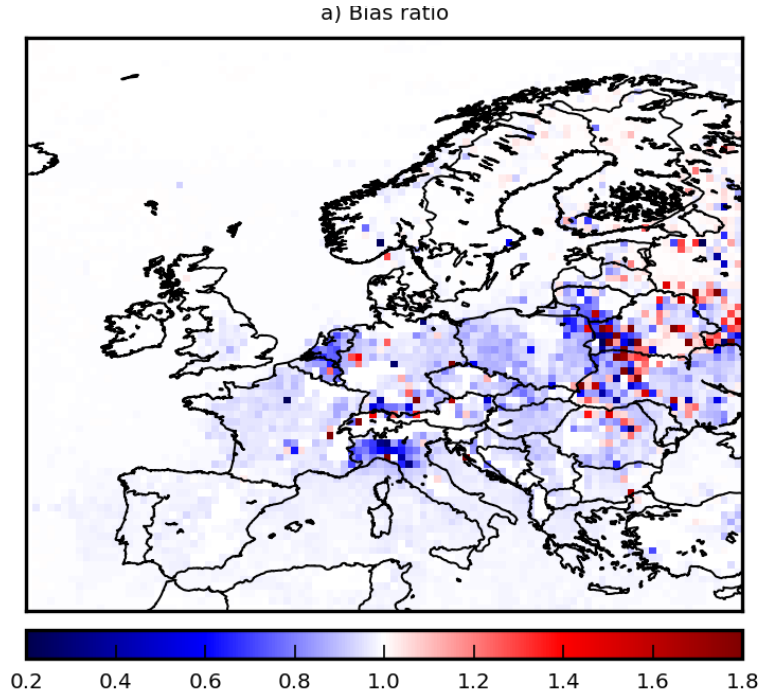


Figure 4. Ratios of the posterior and prior biases between monthly mean surface concentrations from CHIMERE and the MOPITTsuper-observations, in February 2015. All ratios lower than 1, in blue, demonstrate that posterior emission estimates improve the simulation compared to the prior ones.

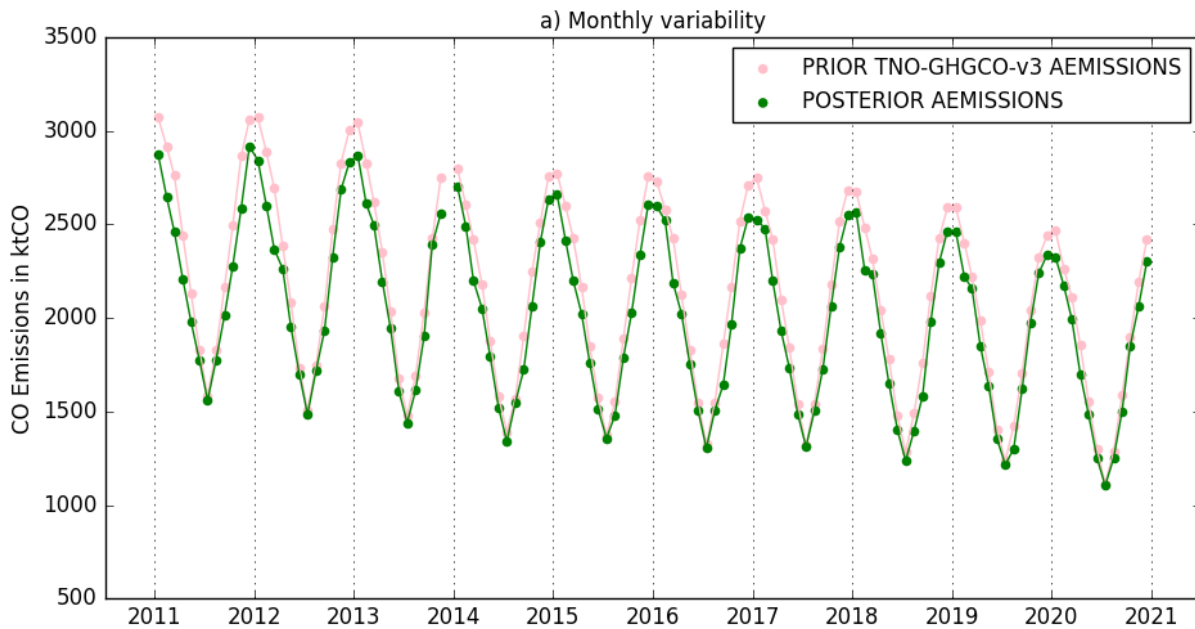


Figure 5. Monthly estimates of the anthropogenic CO emissions from the TNO-GHGco-v3 inventory (in pink) and posterior anthropogenic emission estimates (in green), in ktCO, for the continental domain, from January 2011 to December 2020.

In 2015, the posterior anthropogenic emission estimates for France, Germany, Italy, Poland and Spain are about 5.4%, 7.7%, 12.3%, 6.7%, and 4.1% lower than the prior ones, respectively (Table 5), indicating that the prior TNO-GHGco-v3 European CO emissions could be slightly over-estimated. It conducts to posterior anthropogenic emission estimates about 5.7% lower than the prior emissions for the entire domain in 2015 (Table 5).

Annual and national prior TNO-GHGco-v3 and posterior CO anthropogenic emission estimates in 2015			
Country	CO anthropogenic emissions in ktCO		Increments in %
	Prior TNO-GHGco-v3	Posterior	
France	2203	2084	-5.4
Germany	3297	3044	-7.7
Italy	1996	1750	-12.3
Poland	2377	2217	-6.7
Spain	997	956	-4.1
Entire domain	27926	26332	-5.7

Table 5. Annual and national prior TNO-GHGco-v3 and posterior CO anthropogenic emission estimates in ktCO, and the corresponding relative increments from the inversion in %, for the year 2015.

7. Estimation of European FFCO₂ emissions

7.1. Principle

The long-term strategy envisaged for the estimate of the FFCO₂ emissions based on the CIF and the assimilation of NO₂ and CO (and later CO₂) satellite data should consist in optimizing activity data and emission factors underlying the anthropogenic NO_x, CO and FFCO₂ emissions in the TNO-GHGco inventory rather than the emissions themselves. However, this approach will require some complex developments, tests and analysis while the NO_x and CO emission inversion themselves raised series of technical and scientific challenges to overcome. Therefore, in the context of this final re-analysis of the FFCO₂ emissions in VERIFY, we have followed the simpler "two-step" approach described in D2.11 to convert the information from the NO_x or CO inversions into FFCO₂ emission estimates (Figure 6).

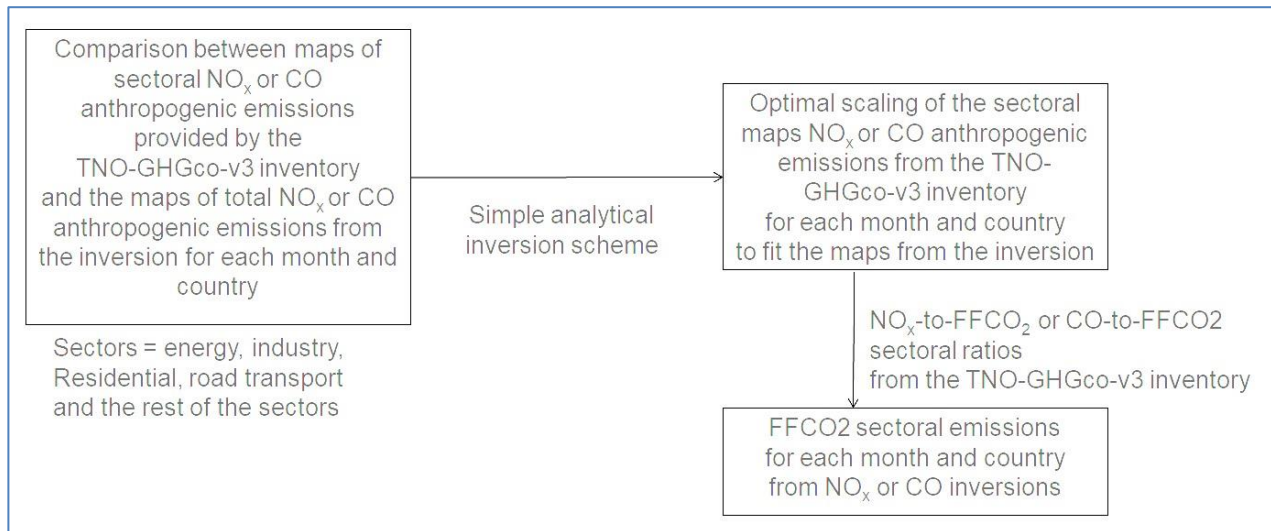


Figure 6. Principle of the "two-step" approach to convert the information from the NO_x inversions or from the CO inversions into FFCO₂ emission estimates.

7.2. Results

The variations of the monthly FFCO₂ emission estimates from the NO_x inversions are shown in Figure 7 for Germany, France, Poland and the Netherlands. The estimates from the inventory and from the inversions for the period 2005 to 2019 are very close to that in D2.11. As a natural consequence of the increase of the NO_x emissions by the inversion and of the use of the emission ratios from the inventory, the inverted FFCO₂ emissions from the NO_x inversions are slightly larger than those from the TNO-GHGco-v3 inventory (Figure 8, Table 6). On the contrary, the FFCO₂ emission estimates derived from the CO inversions are smaller than those from the TNO-GHGco-v3 inventory (Figure 8, Table 6).

As an example for January 2015, the decrease of FFCO₂ emission estimates derived from the CO inversions compared to the inventory is seen for all the sectors, except for Energy (Figure 7). On the contrary, we rather see a slight increase of FFCO₂ emission estimates derived from the NO_x inversions compared to the inventory for all the sectors. Therefore, the inconsistencies between the differences to the inventory from NO_x and CO inversions cannot be easily attributed to the differences in terms of sectoral distribution between the CO and NO_x emissions. For some countries in Central Europe (e.g., Poland, Czech Republic, Hungary), FFCO₂ emission estimates derived from the CO inversions and from the NO_x inversions seem to reflect consistent differences to the inventory with a slight decrease of the FFCO₂ emissions from the NO_x inversions and a strong decrease from the CO inversions (Figure 7). However, our results seem to be incompatible for almost all others countries (and in particular in Spain).

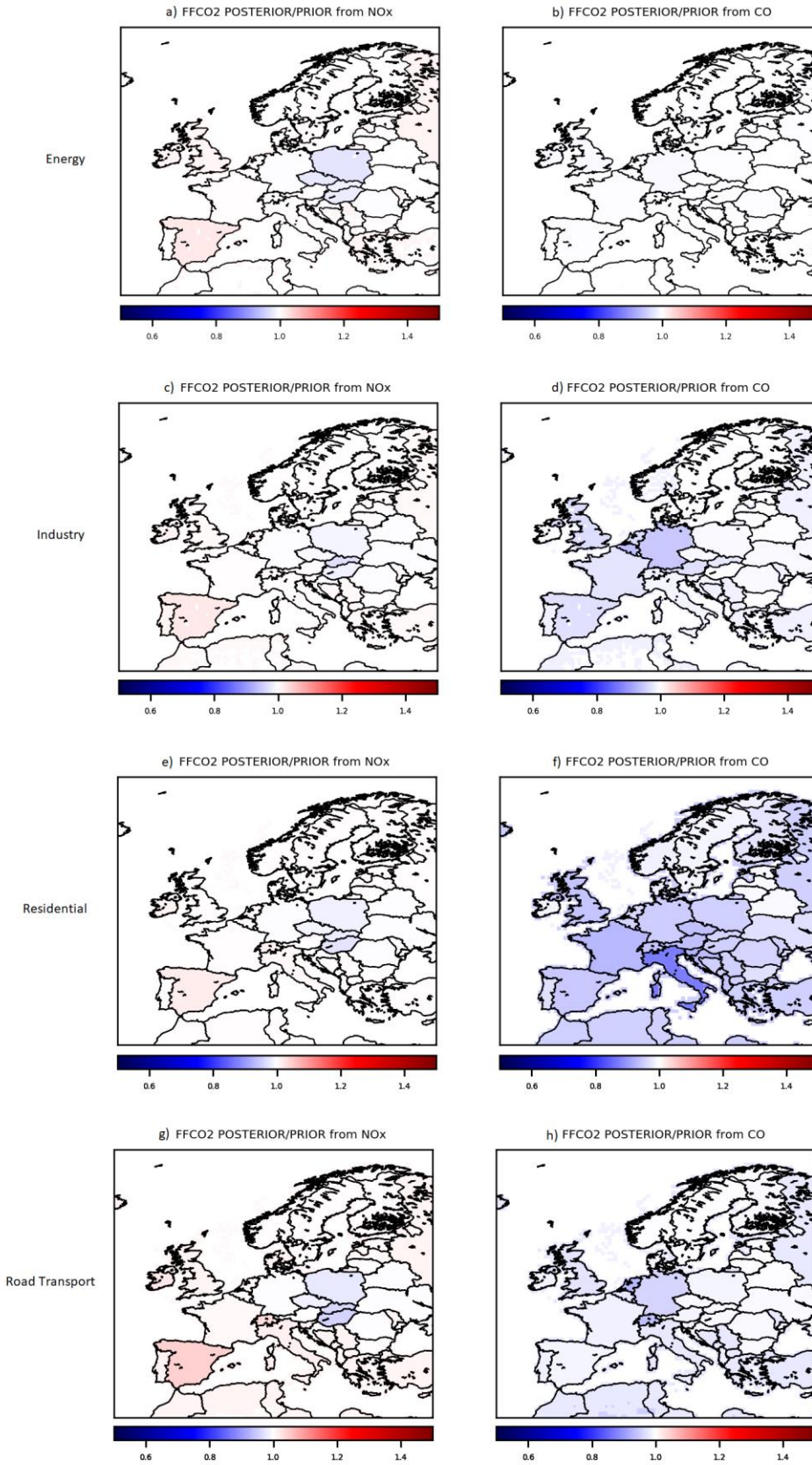


Figure 7. Ratios between the national FFCO₂ emission estimates from the TNO-GHGco-v3 inventory and from the NO_x and CO inversions, for the month of January 2015.

Table 6 lists the FFCO₂ emission estimates from the inventory and from the inversions for 30 European countries in 2015. The weight of the different sectors of activity in the total FFCO₂ emissions is different from that in the anthropogenic NO_x or CO emissions. As a result, the differences in terms of national and annual scale emissions when comparing the results of our analysis and the TNO-GHGco-v3 inventory is generally smaller for FFCO₂ emissions than for NO_x or CO emissions (Table 6). Actually, the differences between the inventory, our FFCO₂ emission estimates from the NO_x inversions and our FFCO₂ emission estimates from the CO inversions are generally weak at national and monthly scales. This could be seen as a positive sign of consistency for the years 2005 to 2019.

However, the lack of decrease of both the NO_x and NO₂-based FFCO₂ inversion estimate when compared to the inventory for the year 2020 raises concerns since the extrapolation of the TNO-GHGco-v3 inventory for the year 2020 likely significantly underestimates the decrease of the emissions due to the covid-19 crisis (see the explanations and analysis in D2.6). Opposed to this, the decrease of the FFCO₂ emission estimates when comparing the results from the CO inversions to the inventory seem quite consistent with the considerations from D2.6 regarding the impact of the covid-19 crisis. D2.6 indicates the difference between the extrapolation of the TNO-GHGco-v3 inventory for 2020 and an estimate assuming "Business As Usual" (BAU) conditions per country is up to -8% while the results from the CAMS_COP079 project indicate it should be up to about -10% (Deliverable D2.6). The difference between the CO-based FFCO₂ emission estimates and the inventory (e.g., -5.5% for Germany, -4.1% for France; see Table 6) would make sense. However, since the emissions in 2019 and previous years are also smaller in the CO-based estimate of the FFCO₂ emissions than in the inventory, the anomaly between these estimates for 2020 and these estimates for the previous years is likely too small.

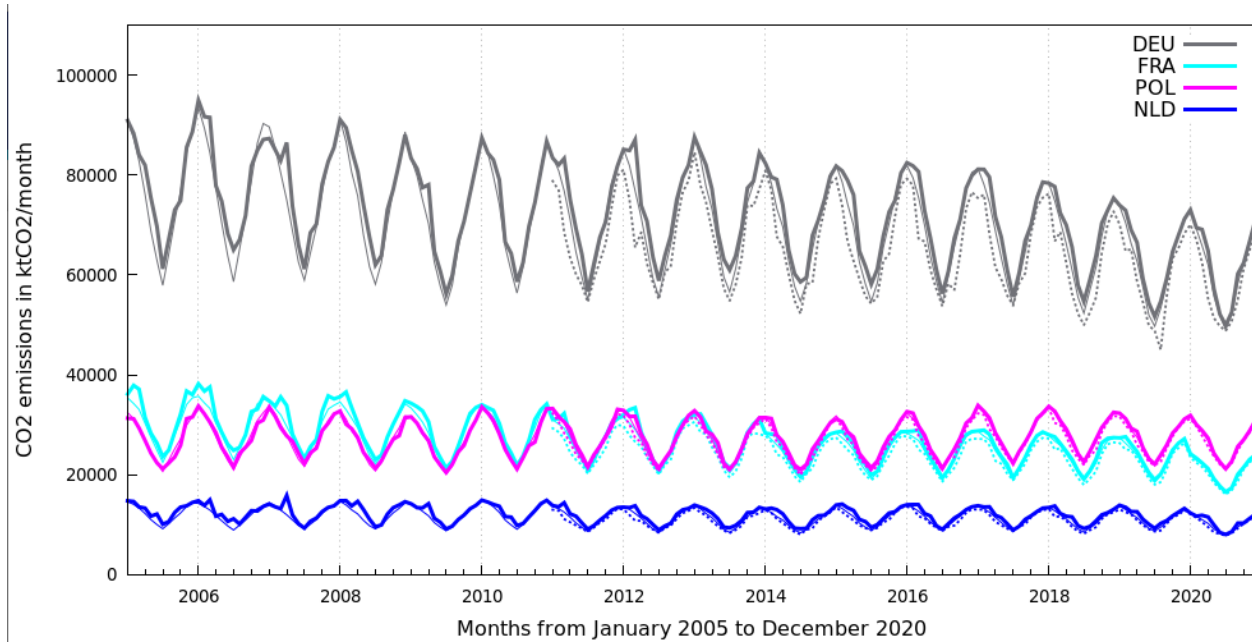


Figure 8. Monthly estimates of German (in grey), French (in cyan), Polish (in magenta) and Dutch (in blue) FFCO₂ emissions from the TNO-GHGco-v3 inventory (in thin line) and from the NO_x inversions (in bold line), in ktCO₂, from January 2005 to December 2020. Monthly estimates of FFCO₂ emissions from the CO inversions are shown in dashed line from January 2011 to December 2020.

Country Code	Difference between NO _x anthropogenic emissions estimates from the inversions and TNO-GHGco-v3 in %	Difference between FFCO ₂ emissions estimates from the NO _x inversions and TNO-GHGco-v3 in %	Difference between CO anthropogenic emissions estimates from the inversions and TNO-GHGco-v3 in %	Difference between FFCO ₂ emissions estimates from the CO inversions and TNO-GHGco-v3 in %
ALB	+1.0	+0.7	-5.9	-2.3
AUT	+3.0	+2.0	-7.9	-5.3
BEL	+3.63	+2.4	-6.2	-5.1
BLR	+0.3	+0.25	-0.6	-0.3
CHE	+5.3	+3.7	-7.6	-6.6
DEU	+4.8	+3.4	-7.7	-5.5
DNK	+1.5	+1.1	-1.2	-0.7
ESP	+4.9	+4.3	-4.1	-2.4
FIN	+0.5	+0.4	-0.5	-0.1
FRA	+3.5	+2.6	-5.4	-4.1
GBR	+2.7	+2.3	-3.5	-2.9
IRL	+0.9	+0.8	-0.8	-0.6
ITA	+5.6	+3.9	-12.3	-5.9

LUX	+3.9	+3.1	-7.2	-6.8
NLD	+9.9	+5.0	-6.8	-3.6
NOR	+0.7	+0.5	-1.1	-0.8
PRT	+3.9	+3.1	-3.0	-2.0
SWE	+0.6	+0.6	-0.4	-0.2
BGR	+1.0	+0.9	-4.0	-0.7
CZE	+1.7	+1.6	-10.6	-2.5
EST	+0.2	+0.2	-0.3	-0.05
HRV	+0.8	+0.6	-7.4	-2.4
HUN	+0.7	+0.4	-7.1	-3.0
LTU	+0.7	+0.3	-0.7	-0.2
LVA	+0.4	+0.3	-0.4	-0.1
POL	+1.3	+1.1	-6.7	-2.3
ROU	+0.3	+0.1	-5.7	-1.6
SVN	+1.8	+1.5	-9.2	-2.4
SVK	+1.2	+0.9	-7.8	-5.3
UKR	-0.2	-0.2	-3.4	-1.6

Table 6. Difference between the anthropogenic NO_x, CO and FFCO₂ annual emissions from TNO-GHGco-v3 and from the inversions, by country, in %, in 2015.

8. Discussion and perspectives for the joint assimilation of NO₂ and CO satellite data

Crossing the information from the CO and NO₂ inversions should help to constrain the FFCO₂ emissions. Nevertheless, as sectoral FFCO₂ emission estimates from NO_x or from CO inversions present contradictory information, the conciliation of these results is challenging at this stage. These results could be explained by the use of anthropogenic NO_x or CO to FFCO₂ emissions ratios from the inventory. Konovalov et al. (2016) indeed indicated that much of the uncertainty in their FFCO₂ emission estimates was associated to these ratios. These results could also be explained by biases in our inversions as highlighted by the concerns raised for the year 2020. In all cases, the derivation of anthropogenic CO₂ estimates that would be based on the joint assimilation of NO₂ and CO satellite data needs further analyses. In particular, the optimization and conversion into FFCO₂ emissions would have required weighting the respective confidence in the NO_x and CO inversions, and in the FFCO₂/anthropogenic NO_x and FFCO₂/anthropogenic CO emission ratios. However, we have not derived estimates of uncertainties in these inversions and emission ratios yet and the current results do not support such a direct synthesis of the current NO_x and CO inversions as discussed below. This demonstrates the need for a better understanding of the uncertainties, and in particular the potential sources of biases in the two inversion processes before attempting at synthesizing the CO and NO₂-based estimates of the FFCO₂ emissions.

Konovalov et al., (2016) have quantified much larger uncertainties in their CO emission estimates than in their NO_x emission estimates. We have highlighted, like them, the lack of sensitivity of satellite CO data to the surface emissions in Europe. Consequently, even if the FFCO₂ emission estimates for 2020 from the CO inversions seems to be more reliable than those from the NO_x inversions, we have more confidence in the FFCO₂ estimates over the full analysis period derived from the NO_x inversions than on those from the CO inversions and our reference inversion based FFCO₂ emission estimates are currently the ones from NO_x inversions.

One of the other perspectives is to consider the availability of co-registered and relatively high (5x3.5 km²) resolution images of CO and NO₂ from the TROPOMI instrument onboard the Sentinel-5P mission since 2018. Such images should provide more potential to constrain the FFCO₂ emissions than the connection between much coarser resolution images from OMI and independent instruments measuring CO like MOPITT. Even though these data do not cover the targeted 15 years period of analysis, demonstrating their potential over 1 or 2 years, and developing techniques to fully exploit them, should strengthen the basis of the co-assimilation of co-emitted species for the monitoring of CO₂ anthropogenic emissions.

9. References

Berchet, A., Sollum, E., Thompson, R. L., Pison, I., Thanwerdas, J., Broquet, G., Chevallier, F., Aalto, T., Berchet, A., Bergamaschi, P., Brunner, D., Engelen, R., Fortems-Cheiney, A., Gerbig, C., Groot Zwaaftink, C. D., Haussaire, J.-M., Henne, S., Houweling, S., Karstens, U., Kutsch, W. L., Lujckx, I. T., Monteil, G., Palmer, P. I., van Peet, J. C. A., Peters, W., Peylin, P., Potier, E., Rödenbeck, C., Saunio, M., Scholze, M., Tsuruta, A., and Zhao, Y.: The Community Inversion Framework v1.0: a unified system for atmospheric inversion studies, *Geosci. Model Dev.*, 14, 5331–5354, <https://doi.org/10.5194/gmd-14-5331-2021>, 2021.

Boersma, K. F., Eskes, H., Richter, A., De Smedt, I., Lorente, A., Beirle, S., Van Geffen, J., Peters, E., Van Roozendaal, M. and Wagner, T.: QA4ECV NO₂ tropospheric and stratospheric vertical column data from OMI (Version 1.1) [Data set], Royal Netherlands Meteorological Institute (KNMI), <http://doi.org/10.21944/qa4ecv-no2-omi-v1.1>, 2017.

Chevallier, F., M. Fisher, P. Peylin, S. Serrar, P. Bousquet, F.-M. Bréon, A. Chédin, and P. Ciais: Inferring CO₂ sources and sinks from satellite observations: method and application to TOVS data, *J. Geophys. Res.*, 110, D24309, [doi:10.1029/2005JD006390](https://doi.org/10.1029/2005JD006390), 2005.

CHIMERE documentation,

<https://www.lmd.polytechnique.fr/chimere/docs/CHIMEREdoc2017.pdf>, Last update of this documentation: June 8, 2017, 2017.

Deeter, M. N., Edwards, D. P., Francis, G. L., Gille, J. C., Mao, D., Martínez-Alonso, S., Worden, H. M., Ziskin, D., and Andreae, M. O.: Radiance-based retrieval bias mitigation for the MOPITT

instrument: the version 8 product, *Atmos. Meas. Tech.*, 12, 4561–4580, <https://doi.org/10.5194/amt-12-4561-2019>, 2019.

Deliverable D2.10, https://verify.lsce.ipsl.fr/images/D210_First_fast-track_Re-analysis_of_the_national_scale_CO2_anthropogenic_emissions_over_2005-2015.pdf, 2019.

Deliverable D2.11, https://verify.lsce.ipsl.fr/images/VERIFY_D211_Second_Re-analysis_of_the_national_scale_CO2_anthropogenic_emissions_over_2005-2015_v1.pdf, 2021.

Deliverable D3.10, https://verify.lsce.ipsl.fr/images/VERIFY_D310_Community_inversion_Framework_v1.pdf, 2021.

EMEP/CEIP,

https://ceip.at/ms/ceip_home1/ceip_home/webdab_emepdatabase/emissions_emepmodels/

Fortems-Cheiney, A. F. Chevallier, I. Pison, P. Bousquet, S. Szopa, M. Deeter, and C. Clerbaux: Ten years of CO emissions as seen from MOPITT, *J. Geophys. Res. Atmospheres*, 116, D5, <https://doi.org/10.1029/2010JD014416>, 2011.

Fortems-Cheiney, A. Chevallier, F., Pison, I., Bousquet, P., Saunois, M., Szopa, S., Cressot, C., Kurosu, T. P., Chance, K., and Fried, A.: The formaldehyde budget as seen by a global-scale multi-constraint and multi-species inversion system, *Atmos. Chem. Phys.*, 12, 6699–6721, <https://doi.org/10.5194/acp-12-6699-2012>, 2012.

Fortems-Cheiney, A., Pison, I., Broquet, G., Dufour, G., Berchet, A., Potier, E., Coman, A., Siour, G., and Costantino, L.: Variational regional inverse modeling of reactive species emissions with PYVAR-CHIMERE-v2019, *Geosci. Model Dev.*, 14, 2939–2957, <https://doi.org/10.5194/gmd-14-2939-2021>, 2021a.

Fortems-Cheiney, A., Broquet, G., Pison, I., Saunois, M., Potier, E., Berchet, A., et al.: Analysis of the anthropogenic and biogenic NO_x emissions over 2008–2017: Assessment of the trends in the 30 most populated urban areas in Europe. *Geophysical Research Letters*, 48, e2020GL092206. <https://doi.org/10.1029/2020GL092206>, 2021b.

Guenther, A., Karl, T., Harley, P., Wiedinmyer, C., Palmer, P. I., and Geron, C.: Estimates of global terrestrial isoprene emissions using MEGAN (Model of Emissions of Gases and Aerosols from Nature), *Atmos. Chem. Phys.*, 6, 3181–3210, <https://doi.org/10.5194/acp-6-3181-2006>, 2006.

Gu, D., Wang, Y., Smeltzer, C., and Boersma, K. F.: Anthropogenic emissions of NO_x over China: Reconciling the difference of inverse modeling results using GOME-2 and OMI measurements, *J. Geophys. Res. Atmos.*, 119, 7732–7740, doi:10.1002/2014JD021644, 2014.

Konovalov, I. B., Beekmann, M., Richter, A., and Burrows, J. P.: Inverse modelling of the spatial distribution of NO_x emissions on a continental scale using satellite data, *Atmos. Chem. Phys.*, **6**, 1747–1770, doi:10.5194/acp-6-1747-2006, 2006.

Konovalov, I. B., Berezin, E. V., Ciais, P., Broquet, G., Zhuravlev, R. V., and Janssens-Maenhout, G.: Estimation of fossil-fuel CO₂ emissions using satellite measurements of "proxy" species, *Atmos. Chem. Phys.*, **16**, 13509–13540, <https://doi.org/10.5194/acp-16-13509-2016>, 2016.

Kuenen, J. J. P., Visschedijk, A. J. H., Jozwicka, M., and Denier van der Gon, H. A. C.: TNO-MACC_II emission inventory; a multi-year (2003–2009) consistent high-resolution European emission inventory for air quality modelling, *Atmos. Chem. Phys.*, **14**, 10963–10976, <https://doi.org/10.5194/acp-14-10963-2014>, 2014.

Levelt, P. F., Joiner, J., Tamminen, J., Veefkind, J. P., Bhartia, P. K., Stein Zweers, D. C., Duncan, B. N., Streets, D. G., Eskes, H., van der A, R., McLinden, C., Fioletov, V., Carn, S., de Laat, J., DeLand, M., Marchenko, S., McPeters, R., Ziemke, J., Fu, D., Liu, X., Pickering, K., Apituley, A., González Abad, G., Arola, A., Boersma, F., Chan Miller, C., Chance, K., de Graaf, M., Hakkarainen, J., Hassinen, S., Ialongo, I., Kleipool, Q., Krotkov, N., Li, C., Lamsal, L., Newman, P., Nowlan, C., Suleiman, R., Tilstra, L. G., Torres, O., Wang, H., and Wargan, K.: The Ozone Monitoring Instrument: overview of 14 years in space, *Atmos. Chem. Phys.*, **18**, 5699–5745, <https://doi.org/10.5194/acp-18-5699-2018>, 2018.

Mailler S., L. Menut, D. Khvorostyanov, M. Valari, F. Couvidat, G. Siour, S. Turquety, R. Briant, P. Tuccella, B. Bessagnet, A. Colette, L. Letinois, and F. Meleux, CHIMERE-2017: from urban to hemispheric chemistry-transport modeling, *Geosci. Model Dev.*, **10**, 2397–2423, <https://doi.org/10.5194/gmd-10-2397-2017>, 2017.

Menut, L., Bessagnet, B., Khvorostyanov, D., Beekmann, M., Blond, N., Colette, A., Coll, I., Curci, G., Foret, G., Hodzic, A., Mailler, S., Meleux, F., Monge, J.-L., Pison, I., Siour, G., Turquety, S., Valari, M., Vautard, R., and Vivanco, M. G.: CHIMERE 2013: a model for regional atmospheric composition modelling, *Geosci. Model Dev.*, **6**, 981–1028, doi:10.5194/gmd-6-981-2013, 2013.

Menut, L., Bessagnet, B., Mailler, S., Pennel, R., Siour, G.: Impact of Lightning NO_x Emissions on Atmospheric Composition and Meteorology in Africa and Europe. *Atmosphere*, **11**, 1128, 2020.

Miyazaki, K., Eskes, H., Sudo, K., Boersma, K. F., Bowman, K., and Kanaya, Y.: Decadal changes in global surface NO_x emissions from multi-constituent satellite data assimilation, *Atmos. Chem. Phys.*, **17**, 807–837, <https://doi.org/10.5194/acp-17-807-2017>, 2017.

Owens, R. G. and Hewson, T.: ECMWF Forecast User Guide, Reading, <https://doi.org/10.21957/m1cs7h>, <https://software.ecmwf.int/wiki/display/FUG/Forecast+User+Guide>, 2018.

Petrescu, A. M. R., McGrath, M. J., Andrew, R. M., Peylin, P., Peters, G. P., Ciais, P., Broquet, G., Tubiello, F. N., Gerbig, C., Pongratz, J., Janssens-Maenhout, G., Grassi, G., Nabuurs, G.-J., Regnier, P., Lauerwald, R., Kuhnert, M., Balkovič, J., Schelhaas, M.-J., Denier van der Gon, H. A. C., Solazzo, E., Qiu, C., Pilli, R., Konovalov, I. B., Houghton, R. A., Günther, D., Perugini, L., Crippa, M., Ganzenmüller, R., Luijkx, I. T., Smith, P., Munassar, S., Thompson, R. L., Conchedda, G., Monteil, G., Scholze, M., Karstens, U., Brockmann, P., and Dolman, A. J.: The consolidated European synthesis of CO₂ emissions and removals for the European Union and United Kingdom: 1990–2018, *Earth Syst. Sci. Data*, 13, 2363–2406, <https://doi.org/10.5194/essd-13-2363-2021>, 2021.

Rayner, P. J., Michalak, A. M., and Chevallier, F.: Fundamentals of data assimilation applied to biogeochemistry, *Atmos. Chem. Phys.*, 19, 13911–13932, <https://doi.org/10.5194/acp-19-13911-2019>, 2019.

Rivier, L., Ciais, P., Hauglustaine, D. A., Bakwin, P., Bousquet, P., Peylin, P., and Klonecki, A.: Evaluation of SF₆, C₂Cl₄, and CO to approximate fossil fuel CO₂ in the Northern Hemisphere using a chemistry transport model, *J. Geophys. Res.*, 111, D16311, [doi:10.1029/2005JD006725](https://doi.org/10.1029/2005JD006725), 2006.

Super, I., Dellaert, S. N. C., Visschedijk, A. J. H., and Denier van der Gon, H. A. C.: Uncertainty analysis of a European high-resolution emission inventory of CO₂ and CO to support inverse modelling and network design, *Atmos. Chem. Phys.*, 20, 1795–1816, <https://doi.org/10.5194/acp-20-1795-2020>, 2020.

Szopa, S., Foret, G., Menut, L., and Cozic, A.: Impact of large scale circulation on European summer surface ozone: consequences for modeling, *Atmospheric Environment*, 43, 1189–1195, [doi:10.1016/j.atmosenv.2008.10.039](https://doi.org/10.1016/j.atmosenv.2008.10.039), 2008.